

Influence of a single disorder parameter on the conduction mechanisms in manganite thin films

P. Orgiani,^{1,2,*} C. Adamo,^{1,2,3} C. Barone,^{1,2} A. Galdi,^{1,2} A. Yu. Petrov,^{1,2} D. G. Schlom,³ and L. Maritato^{1,4,†}

¹*CNR-INFM Coherentia, I-84081 Baronissi, Salerno, Italy*

²*Dipartimento di Fisica, University of Salerno, I-84081 Baronissi, Salerno, Italy*

³*Department of Materials Science and Engineering, The Pennsylvania State University, University Park, Pennsylvania 16802, USA*

⁴*Dipartimento di Matematica ed Informatica, University of Salerno, I-84081 Baronissi, Salerno, Italy*

(Received 20 June 2007; published 16 July 2007)

We have systematically studied the transport properties of colossal magnetoresistance (CMR) manganite films at temperatures of up to 550 K by changing parameters influencing the amount of disorder in the system. Independent of the type and amount of disorder, the resistivity can always be described using a T^α -power law in the ferromagnetic-metallic phase and a thermally activated behavior in the polaronic-insulating phase. A linear correlation between both the value of the α coefficient and the polaron formation energies E_g as a function of the metal-insulator transition temperature T_{MI} has been found. Our results indicate the possibility of describing the transport properties in CMR manganites in terms of a single disorder parameter.

DOI: [10.1103/PhysRevB.76.012404](https://doi.org/10.1103/PhysRevB.76.012404)

PACS number(s): 75.47.Lx, 71.10.-w, 71.30.+h, 71.38.-k

The mixed-valence perovskite manganese oxides are being intensively studied for their striking properties including colossal magnetoresistance (CMR).¹⁻³ Their strong sensitivity to an applied magnetic field around the ferromagnetic-paramagnetic transition point makes these materials attractive for use in applications as magnetic field sensors. Interest in CMR manganites is not, however, confined to possible applications. Their phase diagram is rich and complex, with different orderings [ferromagnetic-metallic (FM), ferromagnetic-insulating, antiferromagnetic, charge ordered] all occurring as single-stabilized or coexisting phases.⁴⁻⁶ Several experiments⁷ have revealed the tendency of manganites to show coexistence of a FM and a paramagnetic insulating (PI) phase.^{5,8-12} In this phase-separation scenario, the disorder plays a very important role. In fact, as widely reported in the literature (Refs. 4-6 and references therein), although a first-order transition is known to separate the two FM and PI phases, the presence of small amount of disorder prevents the systems from being totally FM or totally PI,¹³⁻¹⁷ while, with further increase of disorder, it has been theoretically predicted that the FM-PI transition should again become first order.¹⁸ As pointed out by Dagotto,¹⁹ these studies point out the sensitivity of manganites to disorder, indicating that a disorder strength axis should be incorporated into their phase diagrams and careful investigations should be performed to study its influence on these compounds.^{20,21}

Experimentally, disorder is a difficult quantity to define and control. Different experimental parameters (low-temperature residual resistivity, saturation magnetization, etc.) have been tentatively associated with the disorder present in a system, but none of them is able to afford an absolute determination of this quantity, especially on a nanometric scale. This experimental limitation calls for systematic studies, in which different parameters influencing the disorder can be varied in a controlled way, to investigate the effects on the physical properties of the system. The aim of this Brief Report is to investigate the metal-insulator transition (MIT) in CMR manganites as a function of different types of disorder. In particular, we have systematically studied the low-temperature (below the MIT temperature T_{MI} defined as the temperature at which a peak in the resistivity is

observed) and high-temperature (above T_{MI}) transport properties of CMR manganite films by changing various parameters affecting disorder. These include the oxygen content (i.e., the doping level), the substrate induced epitaxial strain, the divalent cations, and small deviations from stoichiometric composition. All of the experimental findings strongly support the idea that it is indeed possible to correlate the transport properties in CMR manganites with a single, “universal” disorder parameter.

Several substrates are suited to the epitaxial growth of manganite films. In this study, we used (100)SrTiO₃ (STO), (100)LaAlO₃ (LAO), (100)NdGaO₃ (NGO), and (100)MgO (MgO). The samples investigated in this work, La_{0.7}Ba_{0.3}MnO_x (Lbmo) and La_{0.7}Sr_{0.3}MnO₃ (Lsmo) thin films, were deposited by pulsed-laser deposition and by molecular-beam epitaxy (MBE), respectively. Details on the fabrication procedures and the structural characterizations are reported elsewhere.^{22,23} In brief, the main difference among the Lbmo samples is oxygen content. This results in disorder in the electrical doping arising from the disordered oxygen vacancies. The main difference among the Lsmo samples is the variations in their heavy cation stoichiometry. In the Lbmo and Lsmo films grown on different substrates, differences in disorder arise from different lattice mismatches with the substrates and result in elastic deformations of the unit cell, which alter the Mn-O orbital arrangement and their overlap. Some Lsmo films were grown in the form of superlattices on (111) STO substrates using a layer-by-layer MBE technique. In these samples, the Mn atomic planes alternate with either LaO₃ or SrO₃ blocks, removing the structural disorder arising from the random distribution of Sr ions within the films.²⁴

For the Lbmo films grown on STO, the oxygen content is varied by changing the time or the temperature of the post-annealing procedure. The heavy-atom stoichiometry (La:Ba:Mn=0.7:0.3:1) of these samples has been carefully analyzed to be sure that the main difference in the disorder is related to the oxygen vacancies.²² The resistivity vs temperature (up to 550 K) curves for three 20-nm-thick Lbmo films are reported in Fig. 1 (the annealing procedure, along with

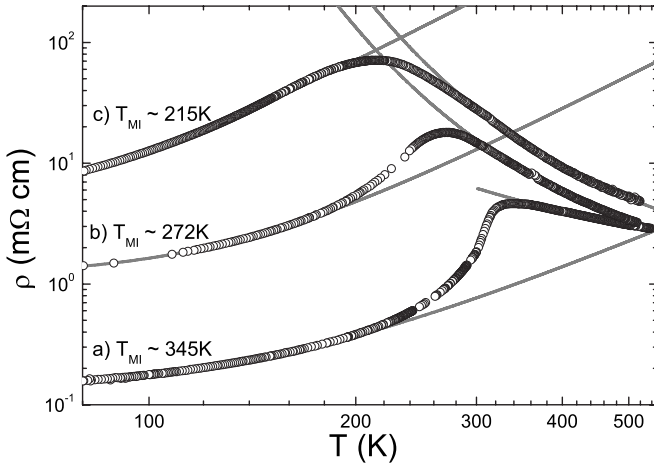


FIG. 1. Resistivity vs temperature behavior of three 20-nm-thick Lbmo films; the curves correspond to three samples showing T_{MI} values of (a) 345 K, (b) 272 K, and (c) 215 K. The metallic ferromagnetic ρ_{FM} and the polaronic ρ_{PI} fitting curves (continuous line at low and high temperatures, respectively) are also reported for all of the samples.

the structural and the transport characterization of these samples, is reported in detail elsewhere²²). They are representative of a larger number of Lbmo samples and show T_{MI} values of 345, 272, and 215 K, corresponding to optimally doped, slightly underdoped, and heavily underdoped Lbmo films, respectively.

Although alternative scenarios, not necessarily related to polaronic localization concepts, have been proposed,¹⁶ the conductivity in the PI phase, above T_{MI} , is generally thought to be dominated by the hopping motion of self-trapped, small, or correlated polarons. According to the literature,^{25,26} the polaronic resistivity ρ_{PI} is given by the formula $\rho_{PI}(T) = T\rho_{\infty} \exp(E_g/k_B T)$, where E_g could be related to the polaronic binding energy E_p through the formula $E_g = E_p/2$.²⁷ On the other hand, in the FM phase, at temperatures below T_{MI} , although much effort has been spent to understand the transport properties of CMR manganites, there is still no agreement on the expected dependence of $\rho(T)$. To obtain a satisfactory fit of the experimental data, several mechanisms have been proposed to be at work in these compounds. These include the combination of the electron-electron and the single-magnon-induced spin-flip scattering (T^2 -power law), the possibility, due to the half-metal character of CMR manganites, of two-magnon scattering ($T^{9/2}$ dependence), the re-appearance of minority spin states at the Fermi energy and their Anderson localization,^{28,29} the scattering with thermally excited magnons³⁰ (T^3 dependence), the importance of spin-wave scattering phenomena³¹ ($T^{7/2}$ dependence), and the interaction with acoustic phonons³² (T^5 dependence).

As recently shown,²⁸ in the FM phase, the resistivity $\rho(T)$ can be described using a generic T^α -power law, which can simulate different scattering processes, helping to reveal the main active one.²⁸ More precisely, in the FM phase, the $\rho(T)$ curves of CMR manganites are better fitted by the formula $\rho_{FM}(T) = \rho_0 + AT^\alpha$ using ρ_0 , A , and α as free fitting parameters.

TABLE I. Fitting parameters for the low-temperature ferromagnetic resistivity $\rho_{FM}(T) = \rho_0 + AT^\alpha$ and the high-temperature thermal-activated polaronic resistivity $\rho_{PI}(T) = \rho_{\infty} T \exp(E_g/k_B T)$. The data refer to the Lbmo films reported in Fig. 1.

Sample	T_{MI} (K)	ρ_0 (mΩ cm)	A (10^{-6})	α	ρ_{∞} ($\mu\Omega$ cm)	E_g (meV)
PLS345	345	0.13	0.79	2.38	86	85.1
PLS272	272	1.14	0.80	2.89	318	131.8
PLS215	215	4.72	1.74	3.24	366	143.6

In analyzing the resistivity data of all the investigated samples, we have, therefore, used the formula $\rho_{PI}(T) = T\rho_{\infty} \exp(E_g/k_B T)$ in the temperature range above T_{MI} , with ρ_{∞} and E_g as free fitting parameters, and the $\rho_{FM}(T)$ expression proposed by Mercone *et al.* for temperatures below T_{MI} . We have varied the fitting temperature range in units of 10 K for both the FM and the PI regions, keeping the lowest- and highest-temperature fitting extremes fixed, respectively. As the temperature range increases, the statistical error on the fitting parameters monotonically decreases, while the χ^2 value remains quite unchanged, until a critical range is reached at which both the χ^2 and the statistical errors abruptly change (the first over 2 orders of magnitude, the latter by a factor of 4–5). The fitting parameters obtained by this procedure for the Lbmo films in Fig. 1 are reported, as an example, in Table I.

The analysis of the curves in Fig. 1 allows us to point out the first important effect about the influence of the disorder on the transport properties of the CMR manganites. If these properties are mainly driven by the coexistence of FM and PI phases, the resistivity $\rho(T)$ should be written as a linear combination of ρ_{FM} and ρ_{PI} . More specifically, the resistivity behavior should be fitted by the formula $\rho(T) = f\rho_{FM} + (1-f)\rho_{PI}$, where ρ_{FM} is the resistivity in the FM phase, ρ_{PI} is the polaron hopping term, and f represents the volume fraction in the FM metallic region.³² Once the FM and the PI resistivity behaviors have been fitted, as previously described, the phase-separation distribution function f can be easily calculated. In Fig. 2, this function is reported for the three Lbmo samples shown in Fig. 1.

The optimally doped Lbmo film shows an f function continuously varying from the two expected values (1 and 0 for the FM and the PI regime, respectively).^{22,32} As the disorder due to the oxygen vacancies increases, however, the f function shows a significant discontinuity (even more evident in the heavily underdoped Lbmo sample). This clearly indicates that the formula $\rho(T) = f\rho_{FM} + (1-f)\rho_{PI}$ is no longer valid. We have observed similar behaviors of the f function when other types of disorder influence the system. As an example, the behavior of the f function is reported in the case of an optimally oxygen-doped Lbmo film deposited on MgO (curve d in Fig. 2). For this sample, the Curie temperature T_C is higher than 300 K, while the T_{MI} temperature is about 200 K, very reduced with respect to the bulk value because of the disorder induced by the substrate strain. From the data in Fig. 2, it is clear that with increasing disorder, an increasing temperature range separating the two phases appears and

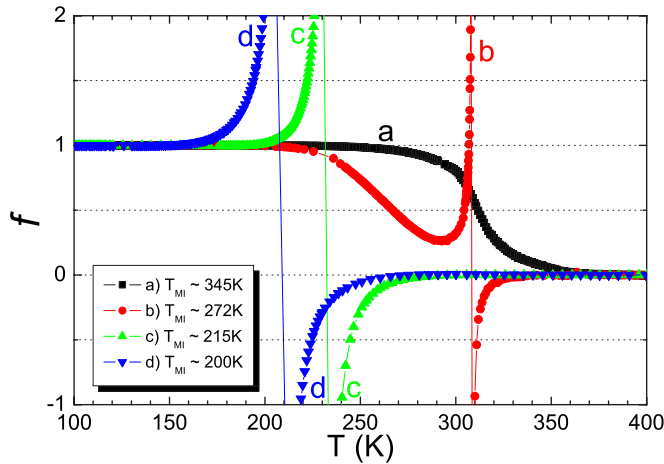


FIG. 2. (Color online) Distribution function f vs temperature behavior for three 20-nm-thick Lbmo films. The curves correspond to the three samples shown in Fig. 1, with T_{MI} values of (a) 345 K, (b) 272 K, and (c) 215 K. The f function for an optimally oxygen-doped Lbmo film grown on MgO substrate is also reported (curve d, with a T_{MI} value of about 200 K).

one cannot describe the transition from one regime into the other using a trivial superimposition of the FM and PI resistivities. This can be related to the restoring of a first-order FM-PI transition with increasing disorder, as theoretically predicted by Salafranca and Brey,¹⁸ or to the influence of the disorder on the size of the FM and PI clusters, shrinking them at very small length scale (nanometers or less) and requiring more complicated quantum mechanical approaches.

From the data in Fig. 1, it is also possible to notice a clear dependence of the measured T_{MI} values with the amount of disorder present in the system. On the other hand, Mercone *et al.*²⁸ already pointed out that for Sr- and Ca-based manganite thin films, the values of the α coefficient depend on the disorder present in the system, evaluated in terms of the values of the residual resistivity. We have, therefore, systematically analyzed the FM transport properties of a large amount of CMR Sr-, Ca-, and Ba-based manganite thin films with different oxygen contents, thicknesses, substrate induced epitaxial strains, and small deviations from the optimal stoichiometric composition. In Fig. 3, the α values obtained for all the investigated samples are shown as a function of the normalized T_{MI}/T_{MI}^{bulk} values, where T_{MI}^{bulk} are the MIT temperatures measured in thick films or bulk materials and are equal to 345, 380, and 270 K, respectively, for the Ba-, Sr-, and Ca-based compounds. Independent of the type of disorder present in the system, the α coefficients appear to be strongly related to the metal insulator-transition temperature T_{MI} .

Even if the source of the disorder is different, increasing the amount of the latter, the metal-insulator temperature T_{MI} decreases and the α coefficient linearly increases for $T_{MI} > 200$ K. In the inset in Fig. 3, the α vs T_{MI} curves at three different stages of the oxygenation (namely, the samples are subsequently postannealed for three different times) are reported for two Lbmo films deposited on STO. For these samples, the assumption that the only changing parameter is

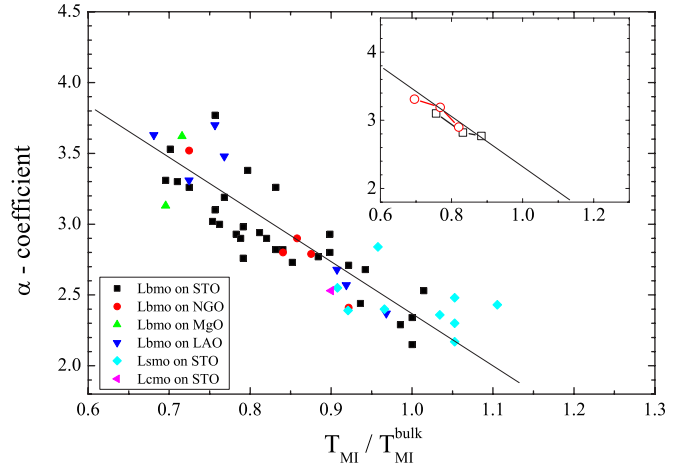


FIG. 3. (Color online) α -coefficient behavior as a function of the metal-insulator-transition temperature T_{MI} for Lbmo films grown on STO (black squares), NGO (red circles), MgO (green up triangles), and LAO (blue down triangles) substrates. The α -coefficient values are also reported for Lsmo films (cyan diamonds) and an Lcmo film (magenta left-triangle) on STO substrates. In the inset, the evolution of the α coefficient at different stages of oxygenation, for two Lbmo films grown on STO substrates, is reported. The dotted lines have the same slope in both graphs.

the oxygen content is strictly verified, and the slopes of both of these curves are the same as that shown in the main figure.

At high temperatures above T_{MI} , in the polaronic scenario, the disorder should also play an important role in the transport properties of CMR manganites. Using the expression of ρ_{PI} , we have fitted the high-temperature (from T_{MI} up to 550 K) $\rho(T)$ curves of a large part of the films in Fig. 3, obtaining the E_g values plotted as a function of T_{MI} in Fig. 4.

The E_g values are almost constant for samples characterized by low values of T_{MI} (inset in Fig. 4). Once again,

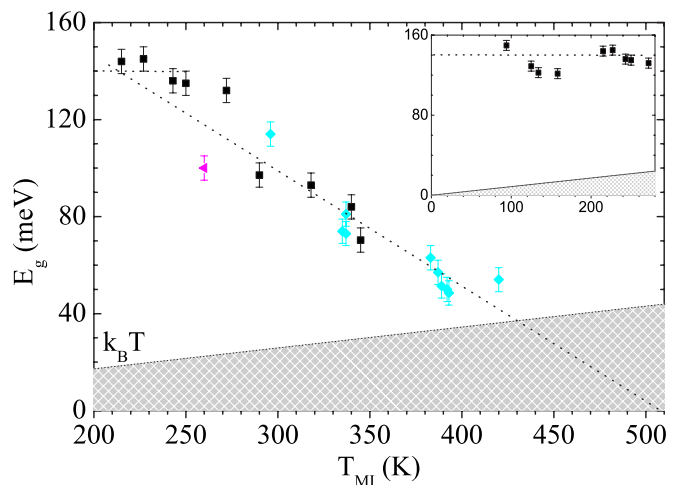


FIG. 4. (Color online) The activation energy E_g versus the metal-insulator transition temperature T_{MI} for Lbmo (black squares), Lsmo (cyan diamonds), and Lcmo (magenta left triangle). The $k_B T$ thermal energy is also plotted as a continuous line. The two lines, describing the E_g vs T_{MI} , are just guides for the eyes.

independent of the type of disorder, for T_{MI} values larger than 200 K, all the obtained E_g values follow a general linear behavior as a function of T_{MI} . As the disorder in the system becomes smaller with increasing T_{MI} values, the E_g values (or, in other terms, the formation energy of a polaron) decrease. For $(\text{LaMnO}_3)_2$ - $(\text{SrMnO}_3)_1$ superlattices grown on (111) STO substrates, in which the ordered sequence of LaO_3 - Mn - LaO_3 - Mn - SrO_3 - Mn blocks (with La:Sr:Mn ratio equal to that of the Lsmo films) removes the disorder associated with a random distribution of Sr ions, the derivative $\Delta\rho/\Delta T \geq 0$ for all the investigated temperatures.²⁴ This is clear evidence that $E_g < k_B T$ (i.e., the thermal energy is larger than the polaronic formation energy). Recently, a linear correlation has been theoretically predicted between the Curie temperature T_C and the squared variance σ^2 of the disorder distribution.¹⁸ Our data (see, for instance, Fig. 4) are in agreement with this model if one assumes that the variance of the trapping-carrier potential distribution is proportional to the average E_g values. This assumption can be intuitively explained considering that, as the disorder increases, the carriers flow in a system where the local trapping potential can be very different, negligible in the case of oxygen octahedrally coordinated Mn atoms and sizable for Mn atoms near one or more oxygen vacancies. Our experimental finding, however, seems to indicate that the MIT temperature T_{MI} and not the Curie temperature T_C is the right parameter to be

associated with the amount of disorder present in the system.

In conclusion, in the limit of small disorder and independent of the type of disorder present, we have found that the phase-separation scenario is verified and the resistivity can be described as a superimposition of FM metallic and PI thermally activated resistivities. As the disorder increases, such a simple assumption is no longer valid, and more complicated models are needed to satisfactorily describe the transition between the two phases. Independent of the type and amount of disorder, in the FM phase, the resistivity can always be described using a generic T^α -power law. A linear correlation between the value of the α coefficient and the metal-insulator transition temperature T_{MI} has been found. In the high-temperature PI regime, the disorder also appears to influence the resistivity behavior. Low-disordered films (showing larger T_{MI} values) are characterized by smaller polaron energies. A linear relationship between the polaron formation energies E_g and the T_{MI} values has been found, again independent of the type of disorder. Our experimental results show that it is possible to describe the transport properties in CMR manganites by a single disorder parameter and that the MIT temperature T_{MI} is a good candidate to play such a role.

The authors are grateful to E. Dagotto for fruitful scientific discussions.

*pasquale.orgiani@na.infn.it

†maritato@sa.infn.it

¹J. M. D. Coey, M. Viret, and S. von Molnar, *Adv. Phys.* **48**, 167 (1999).

²M. B. Salamon and M. Jaime, *Rev. Mod. Phys.* **73**, 583 (2001).

³E. Dagotto, *Nanoscale Phase Separation and Colossal Magnetoresistance* (Springer-Verlag, Berlin, 2002).

⁴E. Dagotto, T. Hotta, and A. Moreo, *Phys. Rep.* **344**, 1 (2001).

⁵A. Moreo, S. Yunoki, and E. Dagotto, *Science* **283**, 2034 (1999).

⁶Y. Tokura and N. Nagaosa, *Science* **288**, 462 (2000).

⁷C. Zener, *Phys. Rev.* **82**, 403 (1951).

⁸A. J. Millis, P. B. Littlewood, and B. I. Shraiman, *Phys. Rev. Lett.* **74**, 5144 (1995).

⁹M. Fäth *et al.*, *Science* **285**, 1540 (1999).

¹⁰K. H. Ahn, T. Lookman, and A. R. Bishop, *Nature (London)* **428**, 401 (2004).

¹¹Ch. Renner *et al.*, *Nature (London)* **416**, 518 (2002).

¹²T. Becker, C. Streng, Y. Luo, V. Moshnyaga, B. Damaschke, N. Shannon, and K. Samwer, *Phys. Rev. Lett.* **89**, 237203 (2002).

¹³S. Yunoki, A. Moreo, and E. Dagotto, *Phys. Rev. Lett.* **81**, 5612 (1998).

¹⁴A. Moreo, M. Mayr, A. Feiguin, S. Yunoki, and E. Dagotto, *Phys. Rev. Lett.* **84**, 5568 (2000).

¹⁵J. Burgy, M. Mayr, V. Martin-Mayor, A. Moreo, and E. Dagotto, *Phys. Rev. Lett.* **87**, 277202 (2001).

¹⁶M. Mayr, A. Moreo, J. A. Verges, J. Arispe, A. Feiguin, and E.

Dagotto, *Phys. Rev. Lett.* **86**, 135 (2001).

¹⁷M. Uehara, S. Mori, C. H. Chen, and S.-W. Cheong, *Nature (London)* **399**, 560 (1999).

¹⁸J. Salafranca and L. Brey, *Phys. Rev. B* **73**, 214404 (2006).

¹⁹E. Dagotto, *Science* **309**, 257 (2005).

²⁰C. Sen, G. Alvarez, and E. Dagotto, *Phys. Rev. B* **70**, 064428 (2004).

²¹Y. Motome, N. Furukawa, and N. Nagaosa, *Phys. Rev. Lett.* **91**, 167204 (2003).

²²P. Orgiani *et al.*, *J. Appl. Phys.* **101**, 033904 (2007).

²³A. Yu. Petrov *et al.*, *Eur. Phys. J. B* **40**, 11 (2004).

²⁴C. Adamo and D. G. Schlom (private communication).

²⁵M. Jaime, M. B. Salamon, M. Rubinstein, R. E. Treece, J. S. Horwitz, and D. B. Chrisey, *Phys. Rev. B* **54**, 11914 (1996).

²⁶M. Jaime *et al.*, *Appl. Phys. Lett.* **68**, 1576 (1996).

²⁷C. A. Perroni, V. Cataudella, G. De Filippis, G. Iadonisi, V. Marioglio Ramaglia, and F. Ventriglia, *Phys. Rev. B* **68**, 224424 (2003).

²⁸S. Mercone *et al.*, *Phys. Rev. B* **71**, 064415 (2005).

²⁹P. Schiffer, A. P. Ramirez, W. Bao, and S.-W. Cheong, *Phys. Rev. Lett.* **75**, 3336 (1995).

³⁰K. Kubo and N. Ohata, *J. Phys. Soc. Jpn.* **33**, 21 (1972).

³¹X. J. Chen, H. U. Habermeier, C. L. Zhang, H. Zhang, and C. C. Almasan, *Phys. Rev. B* **67**, 134405 (2003).

³²G. Li *et al.*, *J. Appl. Phys.* **92**, 1406 (2002).